Formulation of benznidazole-lipid nanocapsules: Drug release, permeability, biocompatibility, and stability studies.

Eva Arrua, Olga Hartwig, Brigitta Loretz, Xabier Murgia, Duy-Khiet Ho, Guillaume Bastiat, Claus-Michael Lehr, Claudio Salomon

Formulation of benznidazole-lipid nanocapsules: Drug release, permeability, biocompatibility, and stability studies.

Eva C. Arrua[a], Olga Hartwig[b,e], Brigitta Loretz[b], Xabier Murgia[b], Duy-Khiet Ho[b], Guillaume Bastiat[c*], Claus-Michael Lehr[b,d*], Claudio J. Salomón[a,e,*]

[a]Institute of Chemistry, IQUIR-CONICET, National Council Research, Suipacha 531, 2000 Rosario, Argentina.

[b]Helmholtz Institute for Pharmaceutical Research Saarland (HIPS), Helmholtz Centre for Infection Research (HZI), Saarland University, 66123 Saarbruecken, Germany.

[c]LUNAM Université, Micro et Nanomédecines Biomimétiques, F-49933 Angers, France; and Inserm, U1066 IBS-CHU, 4 rue Larrey, F-49933 Angers Cédex 9, France.

[d]Department of Pharmacy, Saarland University, 66123 Saarbruecken, Germany.

[e]Pharmacy Department, Faculty of Pharmaceutical and Biochemical Sciences, National University of Rosario, Suipacha 531, 2000 Rosario, Argentina.

* Corresponding author: csalomon@fbioyf.unr.edu.ar

ABSTRACT

Benznidazole, a poorly soluble in water drug, is the first-line medication for the treatment of Chagas disease, but long treatment periods at high dosages cause several adverse effects with insufficient activity in the chronic phase. According to these facts, there is a serious need for novel benznidazole formulations for improving the chemotherapy of Chagas disease. Thus, this work aimed to incorporate benznidazole into lipid nanocapsules for improving its solubility, dissolution rate in different media, and permeability. Lipid nanocapsules were prepared by the phase inversion technique and were fully characterized. Three formulations were obtained with a diameter of 30, 50, and 100 nm and monomodal size distribution with a low polydispersity index and almost neutral zeta potential. Drug encapsulation efficiency was between 83 and 92% and the drug loading was between 0.66 and 1.04%. Loaded formulations were stable under storage for one year at 4 °C. Lipid nanocapsules were found to protect benznidazole in simulated gastric fluid and provide a sustained release platform for the drug in a simulated intestinal fluid containing pancreatic enzymes. The small size and the almost neutral surface charge of these lipid nanocarriers improved their penetration through mucus and such formulations showed a reduced chemical interaction with gastric mucin glycoproteins. LNCs. The incorporation of benznidazole in lipid nanocapsules improved the drug permeability across intestinal epithelium by 10-fold compared with the non-encapsulated drug while the exposure of the cell monolayers to these nanoformulations did not affect the integrity of the epithelium.

KEYWORDS: Neglected tropical diseases, Chagas disease, *Trypanosoma cruzi*, benznidazole, Lipid nanocapsules.

1. **INTRODUCTION**

American Trypanosomiasis, also known as Chagas disease, is a neglected tropical disease caused by the protozoan parasite *Trypanosoma cruzi* (*T. cruzi*) is affecting around 6 to 8 million people worldwide, mostly in Latin America (WHO, 2020). However, owing to human migration, Chagas disease becomes an emerging global health concern spreading into the US, Canada, and European countries (Pinto Dias et al., 2013; Requena-Méndez et al., 2015; Suárez et al., 2022). Acute infection with *T. cruzi* is generally asymptomatic but may develop life-threatening complications during chronic manifestations such as cardiac, neurological, or digestive disorders (Álvarez-Hernández et al. 2021). Currently, only two nitroimidazole derivatives developed in the 1970s are available for Chagas disease: benznidazole (BNZ) and nifurtimox (NFX). With these compounds, the disease is curable if they are prescribed at the early stage of infection (Ribeiro et al., 2020; Vinuesa et al., 2017). BNZ is the first-line treatment, however, prolonged treatment at high dosages may cause several adverse reactions, and, most importantly, the efficacy of BNZ is often reduced in the chronic symptomatic phase of infection after long-term exposure (Chasen et al., 2020). *T. cruzi* is an intracellular parasite and, hence, BNZ needs to penetrate the target organs such as the heart or the colon (Perin et al., 2017). Its mechanism of action requires the activation by trypanosomal type I nitroreductase and involves the production of reactive metabolites within the parasite inhibiting the synthesis of nucleic acids and proteins (Hall et al. 2012). BNZ is available in tablets and the recommended oral dosage is 5-10 mg/kg for pediatric patients and 5-7 mg/kg for adults. Daily doses are in two or three daily administrations for a duration of 30-60 days (Salomon, 2012; Arrúa et al,. 2019). Unfortunately, the currently prescribed treatments require 3 or 4 daily tablets of high doses which often results in high toxicity events, requiring interruption of the chemotherapy. In addition, tablets are not the preferred

pharmaceutical form by certain groups of patients. Taking into account these facts, better delivery strategies using approved drugs and pharmaceutical excipients could help to increase the efficacy, safety, and patient compliance of the current standard treatments for Chagas disease. BNZ is a hydrophobic molecule that shows low aqueous solubility (Santos Souza et al. 2017; de Melo et al., 2018) being more soluble in acetone, methanol, and acetonitrile (Maximiano et al., 2010) as well as in propylene glycol and polyethylene glycol 400 (Santos Souza et al. 2017). Currently, the reduction of the particle size to the nanoscale is an attractive and useful strategy for improving the solubility and dissolution rate of hydrophobic compounds including BNZ (Ferraz et al., 2021; Seremeta et al., 2019; Nhavene et al., 2018; Tessarolo et al., 2018). It is worth mentioning that different BNZ nanoformulations based on lipid excipients were also reported (Morilla et al. 2002; Streck et al., 2019, Mazzeti et al., 2020; Li et al., 2021; Rolon et al., 2022). Considering that novel delivery systems of BNZ are still needed, this study aimed to elucidate if BNZ can be formulated in lipid nanocapsules for improving its solubility, release in different biorelevant dissolution media, and permeability. BNZ-loaded lipid nanocapsules (LNC) of three different sizes were prepared by a phase inversion-based method, eluding organic solvents. LNC were characterized in terms of size, zeta potential, morphology, drug release properties in different biorelevant dissolution media, stability, and storage conditions. Furthermore, LNC biocompatibility was analyzed *in vitro* on the Caco-2 cell line by flow cytometry and confocal microscopy. Finally, LNC interaction with mucin was also investigated.

2. MATERIALS AND METHODS

2.1. Materials

Benznidazole (BNZ; N-benzyl-2-(2-nitroimidazol-1-yl)acetamide; Abarax, lot 9978 A; Laboratorios Elea, Buenos Aires, Argentina) was provided by Instituto Nacional de Parasitología, ANLIS Malbrán, Ministerio de Salud de la Nación, (Buenos Aires, Argentina). Kolliphor® HS 15 (mixture of free PEG 660 and PEG 660 hydroxy stearate) and Lipoid S100 were obtained from BASF SE and Lipoid GmbH (Ludwigshafen, Germany), respectively. Labrafac® WL 1349 (medium-chain triglycerides of caprylic and capric acids) was purchased from Gattefossé S.A. (Saint-Priest, France). Cell culture inserts (Transwell® permeable supports 3460) were obtained from Corning Inc. (Wiesbaden, Germany). Human colon adenocarcinoma cell line Caco-2 (clone HTB-37) was purchased from American Type Culture Collection (ATCC; Rockville, USA), and the cell culture medium, Dulbecco's modified Eagle's medium (DMEM), non-essential amino acids (NEAA), fetal calf serum (FCS), 0.05 % trypsin/EDTA were purchased from Gibco (Carlsbad, USA). Mucins from the porcine stomach (type II), fluorescent dye Nile Red, Dulbecco's phosphate-buffered saline (PBS), Hanks´ balanced salt solution (HBSS), thiazolyl blue tetrazolium bromide (MTT), dimethyl sulfoxide (DMSO) and Triton X-100, 4´,6-Diamidino-2-phenylindole (DAPI) were purchased from Sigma-Aldrich (Darmstadt, Germany). All the other reagents and solvents used in this study were of analytical grade.

2.2. Methods

2.2.1. Preparation and characterization of lipid nanocapsules

LNC were prepared by the phase inversion methodology according to the literature data (Heurtault et al., 2002). Three oil:surfactant ratios were used to produce LNC (see Table

1) of different sizes and surface:volume ratios. Briefly, Lipoid S 100, NaCl, and Kolliphor® HS 15 were added to the Labrafac® WL 1349 oil phase, under stirring at 500 rpm. Then, three cycles of progressive heating and cooling (of 5 minutes each) between 50 °C and 95 °C were performed; during the last cycle in the phase inversion zone, an irreversible shock was induced by dilution with cold water (4 °C). Finally, a slow magnetic stirring (200 rpm) was applied to the nanosuspension for 10 min at room temperature. For drug-loaded LNC, 20 mg of BNZ were dissolved in 1 mL of Labrafac® WL 1349, and the LNC production was performed as described. In a similar procedure fluorescently labeled LNC were obtained by using a lipophilic marker (Nile Red), incorporated in the organic phase (1:10w/w). The particle size and polydispersity index (PDI), and zeta potential (ZP) of LNC were characterized by dynamic light scattering (DLS) using a Nano Particle Analyzer SZ-100 (HORIBA Instruments Inc., Irvine, USA). The samples were prepared by a 60-fold dilution of the LNC with distilled water. All samples were measured in triplicate and are shown as the mean ± standard deviation (SD).

Insert Table 1

2.2.2. Morphological analysis by transmission electron microscopy

Morphological analysis by transmission electron microscopy (TEM) of optimized BNZ-LNC was performed using a Jeol 100CX instrument (JEOL-France, Paris, France). Before analysis, LNC dilutions were carried out (1:120 in water) and were stained using a 2 % phosphotungstic acid aqueous solution and sprayed onto copper grids overlayed with 1 % in chloroform (Mikross, Paris, France). For each grid was employed 1 drop of LNC dilution.

2.2.3. Encapsulation efficiency and loading capacity of benznidazole into lipid nanocapsules

The loading capacity (%LC) and the encapsulation efficiency (%EE) of BNZ into LNC were determined following a reported procedure by Roger et al. (2011). The loaded LNCs were filtered using a Minisart® 0.2 μm filter (Sartorius, Goettingen, Germany) to eliminate the residual components of the lipid formulations. Then, the filtered solutions were diluted at least 10-fold in methanol to release the drug and determine its concentration. BNZ concentration was measured in the supernatant by high-performance liquid chromatography (HPLC), following the methodology described by Morilla et al. (2002). Before the determinations, the effect of the lipid matrix was evaluated and no interferences were detected. On the other hand, unloaded LNC were diluted in the same way as the loaded samples. A 20 μL aliquot of each sample was injected onto the high-performance liquid chromatography (HPLC) column. Measurements were done in triplicate.

The %LC of the BNZ-loaded particles was calculated according to Equation I:

$$\%LC = \frac{W_{BNZ}}{W_{LNC}} \times 100 \qquad \text{Eq. I}$$

Where, W_{BNZ} is the weight of BNZ in the particles and $\boldsymbol{W_{LNC}}$ is the total weight of BNZ-loaded particles obtained.

The *%EE* of the particles was determined according to Equation II:

$$\%EE = \frac{LC_E}{LC_T} \times 100 \qquad \text{Eq. II}$$

Where LC_E and LC_T are the experimental and theoretical loading capacities of the BNZ-loaded particles, respectively.

2.2.4. Evaluation of benznidazole release in simulated gastric and intestinal media

The BNZ release from LNC in different simulated gastric and intestinal media was performed using the dialysis bag method. For that purpose, 5 mg of BNZ or its equivalent of the BNZ-LNC formulation was added to the dialysis bag (cut-off of 12.000 - 14.000 Da) with 10 mL of the simulated gastric medium. The bags were placed in a beaker, and 100 mL of medium was added. The beakers were placed into a thermostatic shaker at 37 °C at 50 rpm. At 0, 1, 2, 3, and 6 hours three aliquots of 1 mL were withdrawn, which were further sterile-filtered and analyzed by HPLC. BNZ release was evaluated in fasted-state simulated gastric fluid (FaSSGF), fed-state simulated intestinal fluid (FeSSIF), and fasted-state simulated intestinal fluid with pancreatic enzymes (FaSSIF+E). Dissolution media were prepared following the literature (Klein, 2010). LNC were diluted 1:2 into simulated fluids and samples were withdrawn for DLS characterization at different time points: 0, 5, 10, 15, 30, 60, 90, and 120 min.

2.2.5. Storage stability of loaded lipid nanocapsules

The stability of the BNZ-LNC was evaluated under two different storage conditions: at room temperature (25 °C) and refrigerator temperature (4 °C). The samples were dispersed in water and were divided into different batches, which were stored at those temperatures. Samples were then withdrawn for DLS characterization after 7 and 15 days of storage, and thereafter, 1, 2, 3, 6, and 12 months after.

2.2.6. Interaction of lipid nanocapsules with mucins

Nanoparticle tracking analysis (NTA, NanoSight, Malvern Instruments, Herrenberg, Germany) was used to determine the interaction between mucus proteins and LNC. The

particle size distribution of Nile Red-labelled LNC (NR LNC) was first characterized by dispersing them in water. The particle size distribution was determined again after mechanically dispersing LNC in a mucin solution containing 0.1 % (w/v) gastric mucins. The Brownian motion of individual LNC under both conditions was tracked by video microscopy using the NTA device, which is equipped with a 532 nm laser and a 565 nm long-pass emission filter for fluorescence detection. By the application of the fluorescence filter, the background noise of auto-fluorescent mucins was removed which allowed the selective visualization of NR LNC in mucin solution. Commercially available carboxyl-terminated polystyrene nanoparticles (NPs) of 100 nm size (red fluorescent FluoSpheres®) were used as a control nanoparticle displaying strong interaction with mucins (Schuster et al., 2013). As described, the same particles coated with a dense layer of polyethylene glycol (PEG) served as a muco-inert control (Ho et al., 2018).

2.2.7. Cell culture of Caco-2 cells

Caco-2 (clone HTB-37), a human intestinal cell line originally derived from colorectal adenocarcinoma, was obtained from American Type Culture Collection (ATCC, Rockville, MD, USA). Caco-2 cells (passages 35-45) were grown in Dulbecco´s Modified Eagle Medium (DMEM, Gibco, Carlsbad, USA). Cell culture medium supplemented with 10% fetal bovine serum (FBS, Sigma-Aldrich, Darmstadt, Germany) and 1 % non-essential amino acids (NEAA, Gibco, Carlsbad, CA, USA). Cells were maintained at 37 °C in a 5 % CO_2 and 95 % humidity atmosphere. Sub-culturing was performed every week with a splitting ratio of 1:20 by using 0.05 % trypsin, and 0.02 % EDTA (Gibco, Carlsbad, CA, USA). The cell culture medium was changed every second day.

2.2.8. Cytotoxicity of lipid nanocapsules in Caco-2 cells

Cell viability was assessed after incubation of Caco-2 cells with LNC by performing a 3-(4,5-dimethylthiazol-2-yl)-2,5-diphenyltetrazolium bromide (MTT) assay. Cells were

seeded in 96 well plates at a density of 20.000 cells per well and grown for 4 days. Afterward, cells were incubated with increasing concentrations of BNZ and BNZ-LNC dispersed in DMEM (0.005, 0.02, 0.2, 0.5, and 2 mg/mL) for 24 hours at 37 °C and 5 % CO_2 on a horizontal shaker. As a positive control, cells were incubated in a cell culture medium corresponding to 100 % viability and, as a negative control, treated with 1 % Triton X-100 in HBSS to induce 0 % cell viability. Cells were washed twice with PBS and MTT reagent (5 mg/mL) was added to the cells and incubated for 4 hours at 37 °C on a horizontal shaker. Afterward, formed formazan crystals were dissolved by adding DMSO, and the absorbance was measured at 550 nm with a plate reader (Infinite M200 PRO, Tecan, Germany). The percentage of viable cells was calculated as previously described and represented as a percentage of untreated cells (100 % viability control) against concentration in [µg/mL] (Nafee et al., 2009). Three independent experiments were performed at least in triplicate.

2.2.9. Epithelial barrier integrity control by transepithelial electrical resistance

Caco-2 cells were grown on porous filter supports (Transwell® Permeable Support 3460, Corning, Wiesbaden, Germany) at a seeding density of 60,000 cells/cm^2 with apical/basolateral medium volumes of 0.5/1.5 mL, respectively. Cells were cultured under submerged conditions until they reached confluence. Transepithelial electrical resistance (TEER) values were measured every day for one week with an epithelial voltohmmeter equipped with STX2 chopstick manual electrodes (EVOM, World Precision Instruments, USA). The raw TEER values were corrected according to the background resistance value of the Transwell® filter and the growth area (1.12 cm^2). Permeation study of BNZ-LNC was performed when Caco-2 cell monolayers displayed a stable epithelial barrier property with TEER values above 1000Ω*cm^2.

2.2.10. Evaluation of cell monolayer permeability of benznidazole lipid nanocapsules

Caco-2 cell monolayers were cultured and submerged onto Transwell® permeable supports as described above (2.2.9). Apical compartments were then washed with PBS and cells were incubated with 100 µL of BNZ LNC solutions or buffer (at a concentration of 30 µg/mL corresponding to BNZ amount of 15 µg/apical compartment), BNZ suspension of 30 µg/mL was served as a control. The paracellular transport of BNZ was determined by sampling 200 µL from the basolateral (acceptor) compartment at various time points (0, 5, 15, 30, 45, 60, 90, 120, 150, 180, 210, and 240 min). The basolateral volume withdrawn at each sampling point was replaced by the same volume of fresh pre-warmed buffer. Throughout the experiment, the cells were incubated at 37 °C and 5 % CO_2 on a horizontal shaker. The amount of BNZ in the acceptor compartment at each time point was assessed by HPLC. The apparent permeability coefficient (P_{app}) of BNZ was then calculated according to Equation III:

$$P_{app} = \left({}^{dQ}/_{dt}\right) * \left({}^{1}/_{C_0 * A}\right) \qquad \text{Eq. III}$$

where ${}^{dQ}/_{dt}$ is the flux (µg/sec) of permeated BNZ, obtained from the slope of the linear region of each permeation profile), A the area of the filter insert (1.12 cm^2), and C_0 the initial donor concentration of BNZ.

2.2.11. Quantitative and qualitative analysis of lipid nanocapsules uptake in Caco-2 cells (flow cytometry and confocal microscopy)

Caco-2 cells were seeded on 24 well plates at a cell density of 60,000 cells per well and cultured for at least 7 days until confluency was reached. Cells were incubated with Nile Red (NR)-labeled LNC as described above (2.2.8). After an incubation period of either 30 min or 1 hour at 37 °C, cells were rinsed twice with PBS to remove remaining nanocapsules, and cells were harvested by trypsin/EDTA. Pelleted cells were re-

suspended in FACS buffer (2 % FCS in HBSS) and analyzed via flow cytometry (FACS Fortessa LSRII; BD Biosciences, Heidelberg, Germany). At least 10.000 cells were recorded for each replicate and the emission of NR-positive cells was collected in the phycoerythrin (PE)-Channel. Mean fluorescence intensity (MFI) was depicted in histograms. Obtained data were analyzed using FlowJo software (FlowJoTM 10.6.0, FlowJo LLC, USA). Three independent experiments were performed at least in triplicates and results are expressed as the mean values ± SD. For microscopic analysis, Caco-2 cells were seeded on 24 well plates at a density of 60,000 cells per well (containing a glass slip) and cultured until reaching confluency. Volumes of 300 µL of the NR-labeled LNC were added to the cells at two different concentrations (20 and 480 µg/mL) and incubated for either 30 min or 1 hour at 37 °C. After incubation, cells were washed twice with PBS, and cell membranes were stained with FITC-conjugated Wheat Germ Agglutinin (WGA; 10µg/mL, Vector Labs, USA). After washing with PBS, cells were fixed with 3 % paraformaldehyde in PBS (PFA, Electron Microscopy Science, USA) for 30 min at room temperature. Then, cell nuclei were stained with 4′,6-diamidino-2-phenylindole (DAPI; 0.1µg/mL) for 15 min, followed by two further washing steps with PBS. Finally, glass slips were mounted onto an objective slide and stored at 4 °C until analysis by confocal laser scanning microscopy (Leica TCS SP 8; Leica, Mannheim, Germany). Images were acquired at 1024 × 1024 resolution, using a 25x water immersion objective (Fluotar VISIR 25x/0.95). Image analysis was performed using LAS X software (Leica Application Suite X; Leica, Mannheim, Germany).

2.2.12. Statistical analysis

All data are shown as mean values ± SD. Statistical analysis was performed in GraphPad Prism 8 (Version 8.2.1.; GraphPad Software, USA).

3. RESULTS AND DISCUSSION

3.1. Physicochemical characterization of loaded lipid nanocapsule formulations

Following a series of preliminary experiments using different lipid excipients, in this study, three different LNC suspensions with different quantities of the same components (Kolliphor® HS 15 and Labrafac®) were prepared by a phase inversion-based method. It is worth noting that the procedure is performed in the absence of organic solvents and involves excipients that are pharmaceutically acceptable and recognized as safe (Dileep et al., 2021). The resulting BNZ-LNC formulations were analyzed by DLS and showed hydrodynamic diameters of approximately 30 nm (28.45 ± 0.04 nm), 50 nm (47.86 ± 0.06 nm), and 100 nm (103.10 ± 0.09 nm), respectively (Table 2).

Insert Table 2

In addition, all LNC showed a monomodal size distribution with a low polydispersity index (PDI ≤ 0.07 in all cases) confirming an excellent uniformity of the LNC, because, in general, PDI values minor than 0.3 indicate a narrow size distribution of nanostructures. Regarding the surface characteristics, a weakly negative ZP with values between -1.59 to -0.96 mV was found, demonstrating an almost neutral surface charge, as described for the preparation of similar lipid nanocarriers (Mouzouvi et al., 2017; Dileep et al., 2021). Corresponding unloaded LNC were of comparable size indicating that BNZ incorporation did not affect the hydrodynamic diameter of the particulates, but slightly changes the surface charge (Table 2). The smallest LNC contained the lowest amount of Labrafac®, whereas the biggest formulation had the highest oil amount (Table 1). Obtained results are in line with previous reports, where the proportion of Labrafac® in the formulation correlated with the average diameter of LNC (Heurtault et al., 2002). The morphology of the prepared systems was visualized by TEM showing a circular

shape for all LNC formulations (Figure 1A-C) and is consistent with the literature data (Heurtault et al., 2002). LNC size was similar to the results obtained by DLS measurements, however, some larger particles were observed for BNZ-LNC 50, possibly formed by a melting process of one or more capsules (Figure 1B). Schematic representations of LNC produced by this method illustrate an oily core of Labrafac® protected by a surfactant cohesive shell consisting of Lipoid S100 anchored in the oily phase and Kolliphor® HS-15 exposed to the water phase (Huynh et al., 2009). Due to BNZ being a hydrophobic molecule, it would possibly be located in the lipophilic core of the LNC. Regarding the encapsulation process, the amount of drug incorporated in the lipid nanostructure is related to both the properties of the drug and the applied methodology. For all particle sizes, it was observed that the drug loading capacity (LC) was between 0.66 and 1.04%, which may be due to the high viscosity of the lipid vehicle, as reported (Li and Yang, 2014). However, other reasons also should be considered including some formulation parameters such as lipid-to-drug ratio, lipid concentration, and processing conditions. It is important to note that low LC was obtained in the formulation of BNZ nanoemulsions (0.3% LC) (Streck et al. 2019) and in the formulation of BNZ vesicles (1% LC) (Li et al, 2021), suggesting that this methodology exhibits such important drawback. Considering that the usual oral dose prescribed for BNZ is between 5 and 7.5 mg/k/day, the lipid ratio and selection and the encapsulation technique should be optimized to increase drug loading for enhancing the therapeutic potential of the encapsulated BNZ. The encapsulation efficiency (EE) was 91.82 % for BNZ-LNC 30), 83.33 % for BNZ-LNC 50), and 87.53 % for BNZ-LNC 100), which is in agreement with the EE values obtained for other hydrophobic drugs encapsulated in similar LNC (Roger et al., 2011; Gamboa et al., 2016).

Insert Figure 1

3.2. Storage stability of lipid nanocapsules at different temperatures

The stability of BNZ-loaded LNC was investigated under two different storage conditions for one year. The produced BNZ-LNC dispersion was stored at room temperature (25 °C) or in the refrigerator (4 °C) and particle size was monitored by DLS. All LNC were physically stable over one year without aggregation when stored at 4 °C, however, storage at room temperature showed few differences between the formulations (Figure 2). Minor changes in mean size were observed for BNZ-LNC 30 all over the assay, but BNZ-LNC 100 seems to be less stable already after 7 days with a size increase to around 150 nm. Medium-sized particles (BNZ-LNC 50) showed the best stability in both conditions compared to the other formulations. By increasing the concentration of Kolliphor® HS-15 more surfactant covers the surface of the LNC avoiding aggregation, however, the behavior of BNZ-LNC 50 could be explained by the most convenient ratio of surfactant to oil (Lamprecht et al., 2002). Despite the slightly negative zeta potential, LNC stability may be improved by the steric repulsion generated by polyethylene glycol (PEG) moieties on the surface (Mouzouvi et al., 2017). In the field of pharmaceutical technology, good physical stability of drug delivery systems is of great interest in terms of manufacturing. According to this, BNZ-LNC 50 would be the best choice regarding thermal and long-term stability.

Insert Figure 2

3.3. Stability in simulated gastric and intestinal media

In the context of oral administration, the *in vitro* stability of LNC was evaluated in simulated gastric and intestinal (GI) media by DLS. Figure 3 shows the size stability of LNC following incubation in fasted-state simulated gastric fluid (FaSSGF; pH 1.6), in

fed-state simulated intestinal fluid (FeSSIF; pH 6.5) and fasted-state simulated intestinal fluid with pancreatic enzymes (FaSSIF+E; pH 6.5). Experimental data comprising particle size and PDI suggests that all LNC formulations were more stable at low gastric and higher (fasted) intestinal pH. In contrast, a certain modification of the colloidal stability was observed with the enzyme-containing fluid. It is important to note that the mean size of the LNC 30 and LNC 100 systems was not affected during the incubation in fasted-state simulated gastric fluid. However, at physiological pH and especially in FaSSIF+E-containing lipases, the nanocapsules become unstable with increasing PDI (Figure 3A/C). Contrary to this, LNC 50 were stable in all simulated GI media with a PDI < 0.3, considering that the formulation was homogenous in size (Figure 3B). This finding could be related to the lipase activity, which is responsible for the fast LNC destabilization in the FaSSIF+E medium where the lipids within the formulation are rapidly digested (Roger et al., 2009).

Insert Figure 3

3.4. Benznidazole release in simulated gastrointestinal media

BNZ shows poor aqueous solubility that may influence its absorption and therapeutic efficacy after oral administration (Davies et al., 2020). As described, the dissolution of hydrophobic compounds is usually affected by the fast and fed state variation (Jantratid et al., 2008). In this regard, *in vivo* performance of solid pharmaceutical preparations can be predicted if the dissolution assay is done in simulated gastrointestinal media (Klein, 2002). Figure 4 summarizes the cumulative release profile of BNZ-loaded LNC in simulated GI media for 6 hours in comparison to the dissolution rate of the BNZ solution. Overall, the sustained release of the encapsulated drug was similar for all three types of

LNC in gastric and intestinal media, with approximately 40 % of the drug in solution after 6 hours (Figure 4A/B). In contrast, the literature describes that more than 95 % of BNZ, formulated as nanocrystals, is released in such conditions after 6 hours (Arrúa et al., 2022). Thus, these results suggest the efficacy of the lipids as carriers to prolong drug release (Lamprecht et al., 2002). A burst release of BNZ was observed in intestinal medium containing pancreatic enzymes, where the biggest LNC formulation (BNZ-LNC 100) released after 1 hour of incubation nearly 50 % of BNZ, BNZ-LNC 50 around 25 %, and the smallest (BNZ-LNC 30) only 15 %, respectively (Figure 4C). As seen, drug release increased by increasing the particle size. It could be due to the higher amount of Labrafac® (LNC 100) which could increase the solubility of the drug, regardless of the size. In addition, the amount of the surfactant (Kolliphor® HS 15) in the LNC could also play a key role in the drug release, because the properties of the barrier of the surfactant could be affected by changing the amount of such excipient. Higher amounts of surfactant might increase the barrier functions slowing the drug release. These observations are positively correlated with the works of Lamprecht et al (2002), and Safwat et al (2017), regarding the relationship between surfactants of the LNC and drug release.

Insert Figure 4

3.5. Interaction of lipid nanocapsules with mucins

Mucus acts as a physical barrier to particles bigger than the mesh spacing of the mucin network (cut-off size of 500 nm). In particular, physicochemical interactions including electrostatic or hydrophobic binding may impede mucus penetration (Murgia et al., 2018). In this context, LNC interaction with mucin glycoproteins was tested by Nanoparticle Tracking Analysis (NTA) which is widely used to determine the size distribution of

nanoparticle (NP) suspensions (Arrua et al., 2021; Christmann et al., 2020). Figure 5 shows the summary of obtained size distributions of Nile Red-labeled LNC (NR-LNC) dispersed in water (without mucins) and in a solution containing 0.1% (w/v) of mucins with representative graphs of NR-LNC compared with carboxylated hydrophobic (mucoadhesive) and PEGylated (muco-inert) control particles of 100 nm size (Figure 5A). A size shift towards higher particle diameter (>1µm) was observed only for the negatively charged polystyrene NPs indicating strong interaction with mucin due to hydrophobic interactions. However, LNC and PEGylated control nanoparticles had an equivalent size distribution in mucin solution compared to water, which is indicative of a lack of mucin interaction. Indeed, all three LNC displayed muco-inert properties with comparable size distributions in presence of mucin proteins, as there was no significant difference ($P > 0.05$) in particle size (Figure 5B). The net neutral zeta potential and hydrophilic PEG moieties on the surface of LNC formulations appear to reduce the potential hydrophobic and electrostatic interactions with mucins. The strong interaction of carboxylated nanoparticles with mucins is attributed to the hydrophobicity of control particles and hydrophobic domains within the mucin fibers (Schuster et al., 2013; Nordgård et al., 2014). In addition, PEG-coating of drug delivery systems will neutralize the particle surface charge and reduce the interaction by shielding hydrophobicity and the capability of hydrogen bonding (Ho et al., 2018; Yang et al., 2012). Herein, LNC showed reduced mucin interactions that may enhance muco-penetration and the capability to reach the cellular targets underneath the mucus barrier.

Insert Figure 5

3.6. Cytotoxicity of lipid nanocapsules in Caco-2 cells

Caco-2, a human epithelial colorectal adenocarcinoma cell line was used for evaluating the biocompatibility of the BNZ-loaded LNC, unloaded LNC, and raw BNZ. Cytotoxicity

was evaluated by the MTT assay. As seen in Figure 6, After 24 h of incubation, both loaded and unloaded LNC showed only a 15 % reduction in cell viability at a concentration of 500 µg/mL, which indicates good cellular tolerance under these experimental conditions. However, data obtained showed an increased cytotoxic effect with increasing concentrations of loaded LNC. In particular, BNZ-LNC 30 showed a cell viability decrease of up to 45%. It was also found that the toxicity increased when the particle size of the LNC decreased suggesting an inverse relationship between the size and toxicity (Leroux et al., 2017). It should be noted that the BNZ solution was less toxic to the cells compared with the loaded nanocapsules while unloaded LNC showed fewer cytotoxic effects than the corresponding loaded LNC (Figure 6). Cytotoxicity of nanocarriers in different cell lines was previously reported and is mainly associated with the non-ionic component within the vehicle (Le Rouxet al., 2017; Maupas et al., 2011).

Insert Figure 6

3.7. Transepithelial electrical resistance

After oral administration, the drug uptake is restricted by the limited permeation through biological barriers, and *in vitro* intestinal models can help to evaluate the *in vivo* rate of absorption of those molecules (Strugari et al., 2018; Zhang et al., 2015). In this context, the integrity and permeability of the cellular monolayer can be elucidated by measuring the transepithelial/transendothelial electrical resistance (TEER) (Srinivasan et al., 2015). Herein, the effects of BNZ-loaded lipid nanocapsules on epithelial barrier function were evaluated on Caco-2 monolayers (see supplementary information Figure S1). This assay indicated that TEER values were similar after incubation with either the different BNZ

nanosystems, suggesting that the barrier properties of the cell monolayers were not affected, which is in agreement with the literature data (Murgia et al., 2017; Arrúa et al., 2021).

3.8. Permeability study of benznidazole lipid nanocapsules in Caco-2 cells

In general, drug-loaded lipid nanocarriers can modulate the drug release as well as improve its permeability (Poletto et al.,2008; Bapat 2019; Michalowski et al., 2020). As described, BNZ is poorly water-soluble and exhibits low permeability (Li et al., 2021; de Jesus et al., 2021) Therefore, the permeability of the BNZ-loaded LNC systems was evaluated across the cellular barrier to elucidate if the drug could reach deeper tissue and combat intracellular *T. cruzi* infection. As observed in Figure 7 the *in vitro* intestinal absorption of BNZ encapsulated in the lipid carrier was higher than that of the drug in solution. After 3 hours, approximately 56.0±0.3 % (BNZ-LNC 30), 51.9±0.2 % (BNZ-LNC 50), and 45.5±0.3 % (BNZ-LNC 100) of BNZ were translocated through the cell layer, and only < 5 % of the free drug (Figure 7A). An almost 10-fold increase of the apical-to-basolateral permeation was obtained for BNZ-loaded LNC in comparison to BNZ alone. Apparent permeability (P_{app}) values for non-encapsulated BNZ were below 2.7±0.1 x 10^{-6}cm/s compared to 3.90±0.02 x 10^{-5}cm/s (BNZ-LNC 30), 3.64±0.05 x 10^{-5}cm/s (BNZ-LNC 50), and 3.44±0.09 x 10^{-5}cm/s (BNZ-LNC 100), respectively (Figure 7B). Thus, its incorporation in these lipid nanostructured systems improves its absorption on proliferating Caco-2 cells, which could be to the increase in BNZ dissolution (Paillard et al., 2010). The smallest LNC size seems to be absorbed faster by the cells and increases the permeation of BNZ in comparison with the other BNZ nanocapsules, suggesting that the size of the nanocarrier plays a fundamental role in the permeation through the mucus barrier, which is consistent with previous studies (Bandi et al., 2020; Arrúa et al., 2021).

Insert Figure 7

4. CONCLUSION

Three novel benznidazole nanocapsules were developed by the phase inversion technique in a size range between 30 and 100 nm and with a very low polydispersity index. The encapsulation efficiency was higher than 88 %, even though the obtained drug loading capacity was less than 1.5 %. Using transmission electron microscopy a circular shape for all the nanoformulations was observed. Physical stability studies confirmed that the loaded nanocapsules were stable under storage, at 4 ^{o}C, keeping their original size for, at least, one year. The dissolution assay demonstrated that these nanocapsules protected the drug in simulated gastric fluid and provided a sustained release platform for benznidazole in a simulated intestinal fluid containing pancreatic enzymes. The physicochemical properties of the developed nanocapsules enhance the penetration through mucosal barriers, showing a small size, a reduced interaction with mucin fibers, and a high cellular uptake in enterocyte-like cells without affecting the integrity of the epithelium. Moreover, LNC formulation increased the permeability of BNZ enhancing the distribution of the drug into deeper tissues to reach target cells. Thus, taking into account that the recommended dose of BNZ by the oral route is between 5 and 7.5 mg/k/day, it is fundamental and necessary to optimize the lipid nanoformulation to increase the drug loading enhancing therapeutic outcomes in the treatment of Chagas disease.

AUTHOR CONTRIBUTIONS: Conceptualization, E.A.; O.H.; D-K. H.; X.M.; methodology, E.A.; O.H.; D-K. H.; X.M.; validation, E.A., O.H.; D-K. H.; X.M.; investigation, E.A.; O.H.; D-K. H.; X.M.; resources, G.B.; C-M.L.; C.S.; data curation, E.A.; O.H.; D-K. H.; X.M.; writing—original draft preparation, E.A.; O.H.; D-K. H.;

X.M.; writing—review and editing, X.M., G.B.; C-M.L.; C.S: supervision, G.B.; C-M.L.; C.S: funding acquisition, G.B.; C-M.L.; C.S. All authors have read and agreed to the published version of the manuscript.

CONFLICTS OF INTEREST: The authors declare no conflict of interest.

ACKNOWLEDGEMENTS AND FUNDING

The authors acknowledge financial support from the Universidad Nacional de Rosario (U.N.R., Rosario, Argentina), Consejo Nacional de Investigaciones Científicas y Técnicas (CONICET, Argentina), Deutscher Akademischer Austauschdienst (DAAD, Deutschland) and the ECOS-SUD ARGENTINA PROGRAM. E.A. thanks to CONICET for a Ph.D. fellowship. O.H. thanks to the EU Horizon 2020 research and innovation program under grant Agreement N° 720905-2.

REFERENCES

D. A. Álvarez-Hernández, R. García-Rodríguez-Arana, A. Ortiz-Hernández, M. Álvarez-Sánchez, M. Wu, R. Mejia, L. A. Martínez-Juárez, A. Montoya, H. Gallardo-Rincon, R. Vázquez-López, A. M. Fernández-Presas. A systematic review of historical and current trends in Chagas disease. Ther Adv Infect Dis. 8 (2021), 20499361211033715.

E. C. Arrúa, K. P. Seremeta, G. R. Bedogni, N. B. Okulik, C. J. Salomon. Nanocarriers for effective delivery of benznidazole and nifurtimox in the treatment of Chagas disease: A review. Acta Trop. 198 (2019), pp. 105080.

E. C. Arrua, O. Hartwig, D. K. Ho, B. Loretz, X. Murgia, C. J. Salomon, C. M. Lehr. Surfactant-free glibenclamide nanoparticles: Formulation, characterization and evaluation of interactions with biological barriers. Pharm Res. 38 (2021), pp. 1081-1092.

E. C. Arrua, O. Hartwig, B. Loretz, H. Goicoechea, X. Murgia, C. M. Lehr, C. J. Salomon. Improving the oral delivery of benznidazole nanoparticles by optimizing the formulation parameters through a design of experiment and optimization strategy. Colloids Surf B Biointerfaces. 217 (2022), pp. 112678.

S. P. Bandi, Y. S. Kumbhar, V. V. K. Venuganti. Effect of particle size and surface charge of nanoparticles in penetration through intestinal mucus barrier. J Nanoparticle Res. 22 (2020), pp. 62.

P. Bapat, R. Ghadi, D. Chaudhari, S. S. Katiyar, S. Jain. Tocophersolan stabilized lipid nanocapsules with high drug loading to improve the permeability and oral bioavailability of curcumin. Int J Pharm. 560 (2019), pp 219-227.

N. M. Chasen, I. Coppens, R. D. Etheridge. Identification and Localization of the First Known Proteins of the *Trypanosoma cruzi* Cytostome Cytopharynx Endocytic Complex. Front Cell Infect Microbiol Frontiers. 9 (2020), pp. 445.

C. Davies, A. Simonazzi, J.F. Micheloud, P.G. Ragone, A.G. Cid, O.S. Negrette, J.M. Bermúdez, L.A. Parada. J Parasitol. 106 (2020), pp. 323–333.

L. R. de Moura Ferraz, A. E. G. A. Tabosa, D. D. S. da Silva Nascimento, A. S. Ferreira, J. Y. R. Silva, S. Alves Jr, L. A. Rolim, P. J. Rolim-Neto. Benznidazole in vitro dissolution release from a pH-sensitive drug delivery system using Zif-8 as a carrier. J Mater Sci: Mater Med 32 (2021), pp, 59.

G. V. U. U. Gamboa, S. D. Palma, A. Lifschitz, M. Ballent, C. Lanusse, C. Passirani, J.

P. Benoit, D. A. Allemandi. Ivermectin-loaded lipid nanocapsules: toward the development of a new antiparasitic delivery system for veterinary applications. Parasitol Res. 115 (2016), pp. 1945–1953.

B. S. Hall, S. R. Wilkinson. Activation of benznidazole by trypanosomal type I nitroreductases results in glyoxal formation. Antimicrob Agents Chemother. 56 (2012), pp. 115-123.

B. Heurtault, P. Saulnier, B. Pech, J. E. Proust, J. P. Benoit. A novel phase inversion-based process for the preparation of lipid nanocarriers. Pharm Res. 19 (2002), pp. 875-80.

D-K. Ho, S. Frisch, A. Biehl, E. Terriac, C. De Rossi, K. Schwarzkopf K, F. Lautenschläger, B. Loretz, X. Murgia, C-M. Lehr. Farnesylated Glycol Chitosan as a Platform for Drug Delivery: Synthesis, Characterization, and Investigation of Mucus–Particle Interactions. Biomacromolecules. 19 (2018), pp. 3489–3501.

D. K. Ho, R. Christmann, X. Murgia, C. De Rossi, S. Frisch, M: Koch, U. F. Schaefer, B. Loretz, D. Desmaele, P. Couvreur, C-M. Lehr. Synthesis and Biopharmaceutical Characterization of Amphiphilic Squalenyl Derivative Based Versatile Drug Delivery Platform. Front Chem. 9 (2020), pp. 1–14.

N. T. Huynh, C. Passirani, P. Saulnier, J. P. Benoit. Lipid nanocapsules: A new platform for nanomedicine. Int J Pharm. 379 (2009), pp. 201–209.

E. Jantratid, N. Janssen, C. Reppas, J.B. Dressman. Dissolution media simulating conditions in the proximal human gastrointestinal tract: an update. Pharm. Res. 25 (2008) 1663–1676.

S. M. de Jesus, L. Pinto, F. L. Moreira, G. H. B. Nardotto, R. Cristofoletti, L. Perin, K.

D. S. Fonseca, P. Barbêdo, L. C. Bandeira, P. M. A. Vieira, C. M. Carneiro. Pharmacokinetics of Benznidazole in Experimental Chronic Chagas Disease Using the Swiss Mouse-Berenice-78 *Trypanosoma cruzi* Strain Model. Antimicrob Agents Chemother. 65 (2021), e01383-20.

S. Klein. The use of biorelevant dissolution media to forecast the in vivo performance of a drug. AAPS J. 12 (2010), pp. 397-406.

A. Lamprecht, Y. Bouligand, J. P. Benoit. New lipid nanocapsules exhibit sustained release properties for amiodarone. J Control Release. 84 (2002), pp. 59–68.

G. Le Roux, H. Moche, A. Nieto, J. P. Benoit, F. Nesslany, F. Lagarce. Cytotoxicity and genotoxicity of lipid nanocapsules. Toxicol Vitr. 41 (2017), pp. 189–199.

Y. Li, L. Yang. Driving forces for drug loading in drug carriers. J Microencapsul. 32 (2015), pp. 255-72.

X. Li, S. Yi, D. B. Scariot, S. J. Martinez, B. A. Falk, C. L. Olson, P. S. Romano, E. A. Scott, D. M: Engman. Nanocarrier-enhanced intracellular delivery of benznidazole for treatment of *Trypanosoma cruzi* infection. JCI Insight. 6 (2021), (9):e145523.

C. Maupas, B. Moulari, A. Béduneau, A. Lamprecht, Y. Pellequer. Surfactant dependent toxicity of lipid nanocapsules in HaCaT cells. Int J Pharm. 411 (2011), pp. 136–141.

F. P. Maximiano, G. H. Y. Costa; J. de Souza, M. S. S. da Cunha-Filho. Caracterização físico-química do fármaco antichagásico benznidazol. Quim. Nova, 33 (2010), pp. 1714-1719.

A. L. Mazzeti, L. T. Oliveira, K. R. Gonçalves, G. C. Schaun, V. C. F. Mosqueira, M. T. Bahia. Benznidazole self-emulsifying delivery system: A novel alternative dosage form

for Chagas disease treatment. Eur J Pharm Sci. 30 (2020), pp. 105234.

P. N. de Melo, L. B. de Caland, M. F. Fernandes-Pedrosa, A. A. da Silva-Júnior. Designing and monitoring microstructural properties of oligosaccharide/co-solvent ternary complex particles to improve benznidazole dissolution. J Mater Sci. 53 (2018), pp. 2472–2483.

C. B. Michalowski, M. D. Arbo, L. Altknecht, A. N. Anciuti, A. S. G. Abreu, L. M. R. Alencar, A. R. Pohlmann, S. C. Garcia, S. S. Guterres SS. Oral treatment of spontaneously hypertensive rats with captopril-surface functionalized furosemide-loaded multi-wall lipid-core nanocapsules. Pharmaceutics. 12 (2020), 80.

M. J. Morilla, P. Benavidez, M. O. Lopez, L. Bakas, E. L. Romero. Development and in vitro characterization of a benznidazole liposomal formulation. Int J Pharm. 249 (2002), pp. 89–99.

C. R. A. Mouzouvi, A. Umerska, A. K. Bigot, P. Saulnier. Surface active properties of lipid nanocapsules. PLoS One, 12 (2017), e0179211.

X. Murgia, H. Yasar, C. Carvalho-Wodarz, B. Loretz, S. Gordon, K. Schwarzkopf, U. Schaefer, C-M. Lehr. Modelling the bronchial barrier in pulmonary drug delivery: A human bronchial epithelial cell line supplemented with human tracheal mucus. Eur J Pharm Biopharm. 118 (2017), pp. 79–88.

X. Murgia, B. Loretz, O. Hartwig, M. Hittinger, C-M. Lehr. The role of mucus on drug transport and its potential to affect therapeutic outcomes. Adv Drug Deliv Rev. 124 (2018), pp. 82–97.

N. Nafee, M. Schneider, U. F. Schaefer, C-M. Lehr. Relevance of the colloidal stability of chitosan/PLGA nanoparticles on their cytotoxicity profile. Int J Pharm. 381 (2009), pp.

130–139.

E. P. F. Nhavene, W. M. da Silva, R. R. Trivelato Jr, P. L. Gastelois, T. Venâncio, R. Nascimento, R. J. C. Batista, C. R. Machado, W. A. de Almeida Macedo, E. M: B. de Sousa. Chitosan grafted into mesoporous silica nanoparticles as benznidazole carrier for Chagas disease treatment. Microporous and Mesoporous Materials, 272 (2018), pp. 265-275,.

C. T. Nordgård, U. Nonstad, M. Ø. Olderøy, T. Espevik, K. I. Draget. Alterations in Mucus Barrier Function and Matrix Structure Induced by Guluronate Oligomers. Biomacromolecules 15 (2014), pp. 2294–2300.

A. Paillard, F. Hindré, C. Vignes-Colombeix, J. P. Benoit, E. Garcion. The importance of endo-lysosomal escape with lipid nanocapsules for drug subcellular bioavailability. Biomaterials 31 (2010), pp. 7542–7554.

L. Perin, R. M. da Silva, K. da S. Fonseca, J. M. de O. Cardoso, F. A. S. Mathias, L. E. S. Reis, I. Molina, R. Correa-Oliveira, P. M. de Abreu Vieira, C. M. Carneiro. Pharmacokinetics and Tissue Distribution of Benznidazole after Oral Administration in Mice. Antimicrob Agents Chemother. 61 (2017), e02410-16.

J. C. Pinto Dias. Human Chagas disease and migration in the context of globalization: Some particular aspects. J. Trop. Med. 2013 (2013), pp. 789758.

F. S. Poletto, E. Jäger, L. Cruz, A. R. Pohlmann, S. S. Guterres. The effect of polymeric wall on the permeability of drug-loaded nanocapsules. Mater Sci Eng C. 28 (2008), pp. 472-478.

A. Requena-Méndez, E. Aldasoro, E. de Lazzari, E. Sicuri, M. Brown, D. A. J. Moore, J. Gascon, J. Muñoz. Prevalence of Chagas Disease in Latin-American Migrants Living in

Europe: A Systematic Review and Meta-analysis. PLoS Negl Trop Dis. 9 (2015), e0003540.

V. Ribeiro, N. Dias, T. Paiva, L. Hagström-Bex, N. Nitz, R. Pratesi R, M. Hecht. Current trends in the pharmacological management of Chagas disease. Int J Parasitol Drugs Drug Resist. 12 (2020), pp. 7–17.

E. Roger, F. Lagarce, J. P. Benoit. The gastrointestinal stability of lipid nanocapsules. Int J Pharm. 379 (2009), pp. 260–265.

E. Roger, F. Lagarce, J.P. Benoit. Development and characterization of a novel lipid nanocapsule formulation of Sn38 for oral administration. Eur J Pharm Biopharm. 79 (2011), pp. 181-188.

M. Rolon, E. Hanna, C. Vega, C. Coronel, M. A. Dea-Ayuela, D. R. Serrano, A. Lalatsa. Solid Nanomedicines of Nifurtimox and Benznidazole for the Oral Treatment of Chagas Disease. Pharmaceutics 14 (2022), pp. 1822.

C. J. Salomon. First Century of Chagas' Disease: An Overview on Novel Approaches to Nifurtimox and Benznidazole Delivery Systems. J Pharm Sci. 101 (2012), pp. 888–894.

H. F. Santos Souza, D. Real, D. Leonardi, S. C. Rocha, V. Alonso, E. Serra, A. M. Silber, C. J. Salomon. Development and in vitro/in vivo evaluation of a novel benznidazole liquid dosage form using a quality-by-design approach. Tropical Medicine and International Health 12 (2017), pp. 1514-1522.

S. Safwat, R. M. Hathout, R. A. Ishak, R.A., N. D. Mortada. Augmented simvastatin cytotoxicity using optimized lipid nanocapsules: a potential for breast cancer treatment. J Liposome Res., 27 (2017), pp. 1–10.

K. P. Seremeta, E. C. Arrúa, N. B. Okulik, C. J. Salomon. Development and characterization of benznidazole nano- and microparticles: A new tool for pediatric treatment of Chagas disease? Colloids Surf. B. 177 (2019), pp. 169-177.

B. S. Schuster, J. S. Suk, G. F. Woodworth, J. Hanes. Nanoparticle diffusion in respiratory mucus from humans without lung disease. Biomaterials. 34 (2013), pp. 3439–3446.

B. Srinivasan, A. R. Kolli, M. B. Esch, H. E. Abaci, M. L. Shuler, J. J. Hickman. TEER measurement techniques for in vitro barrier model systems. J Lab Autom. 20 (2015), pp. 107-126.

L. Streck, V. H. V. Sarmento, R. P. R. P. B. de Menezes, M. F. Fernandes-Pedrosa, A. M. C. Martins, A. A. da Silva-Júnior. Tailoring microstructural, drug release properties, and antichagasic efficacy of biocompatible oil-in-water benznidazole-loaded nanoemulsions. Int J Pharm. 555 (2019), pp. 36-48.

A. Strugari, M. Stan, S. Gharbia, A. Hermenean, A. Dinischiotu. Characterization of nanoparticle intestinal transport using an in vitro co-culture model. Nanomaterials 9 (2018), 5.

C. Suárez, D. Nolder, A. García-Mingo, D. A. J. Moore, P. L. Chiodini. Diagnosis and Clinical Management of Chagas Disease: An Increasing Challenge in Non-Endemic Areas. Res Rep Trop Med. 13 (2022), pp. 25-40

L. D. Tessarolo, R. P. R. P. B. de Menezes, C. P. Mello, D. B. Lima, E. P. Magalhães, E. M. Bezerra, F. A. M. Sales, I. L. Barroso Neto, M. F. Oliveira, R. P. Dos Santos, E. L. Albuquerque, V. N. Freire, A. M. Martins. Nanoencapsulation of benznidazole in calcium carbonate increases its selectivity to *Trypanosoma cruzi*. Parasitology. 145 (2018), pp. 1191-1198.

D. Urimi, R. Widenbring, R. O. Pérez García, L. Gedda, K. Edwards, T. Loftsson, N. Schipper. Formulation development and upscaling of lipid nanocapsules as a drug delivery system for a novel cyclic GMP analog intended for retinal drug delivery. Int J Pharm. 602 (2021), 120640.

T. Vinuesa, R. Herráez, L. Oliver, E. Elizondo, A. Acarregui, A. Esquisabel, J. L. Pedraz, N. Ventosa, J. Veciana, M. Viñas. Benznidazole Nanoformulates: A Chance to Improve Therapeutics for Chagas Disease. Am J Trop Med Hyg. 07 (2017), pp. 1469-1476.

World Health Organisation. Chagas disease (also known as American trypanosomiasis). In: Chagas Disease Fact Sheets. 2020 p. 6. Available: https://www.who.int/news-room/fact-sheets/detail/chagas-disease-(American-trypanosomiasis)

X. Yang, K. Forier, L. Steukers, S. Van Vlierberghe, P. Dubruel, K. Braeckmans K, S. Glorieux, H. J. Nauwynck. Immobilization of Pseudorabies Virus in Porcine Tracheal Respiratory Mucus Revealed by Single Particle Tracking. PLoS One. 7 (2012), e51054.

J. Zhang, C. J. Field, D. Vine, L. Chen. Intestinal uptake and transport of vitamin B12-loaded soy protein nanoparticles. Pharm Res. 32 (2015), pp. 1288-1303.

Table 1. Composition of lipid nanocapsule formulations

LNC	Quantity (mg)				Quantity (mL)	
	Kolliphor® HS-15	Lipoid S-100	NaCl	Labrafac® WL 1349	H_2O	H_2O (4°C)
A	1934	75	156	846	4.055	3
B	846	75	156	1028	2.962	5
C	484	75	156	1209	3.143	5

Table 2. Characterization of lipid nanocapsules (LNCs).

	LNC	Size (nm)	PDI	ZP (mV)	EE (%)
Without BNZ	30	30.33±0.5	0.090±0.05	-7.93±0.2	-
	50	58.14±0.3	0.040±0.04	-5.44±0.8	-
	100	119.57±0.7	0.120±0.08	-6.79±0.6	-
With BNZ	30	28.45±0.4	0.049±0.05	-0.956±0.3	91.82±1.03
	50	47.86±0.6	0.039±0.07	-0.858±0.4	83.33±2.00
	100	103.10±0.9	0.071±0.04	-1.59±0.6	87.53±1.12

PDI: polydispersity index, ZP: zeta potential, and encapsulation efficacy (EE) of benznidazole (BNZ) into LNCs. The mean ± SD of n=9 from three independent experiments is shown.

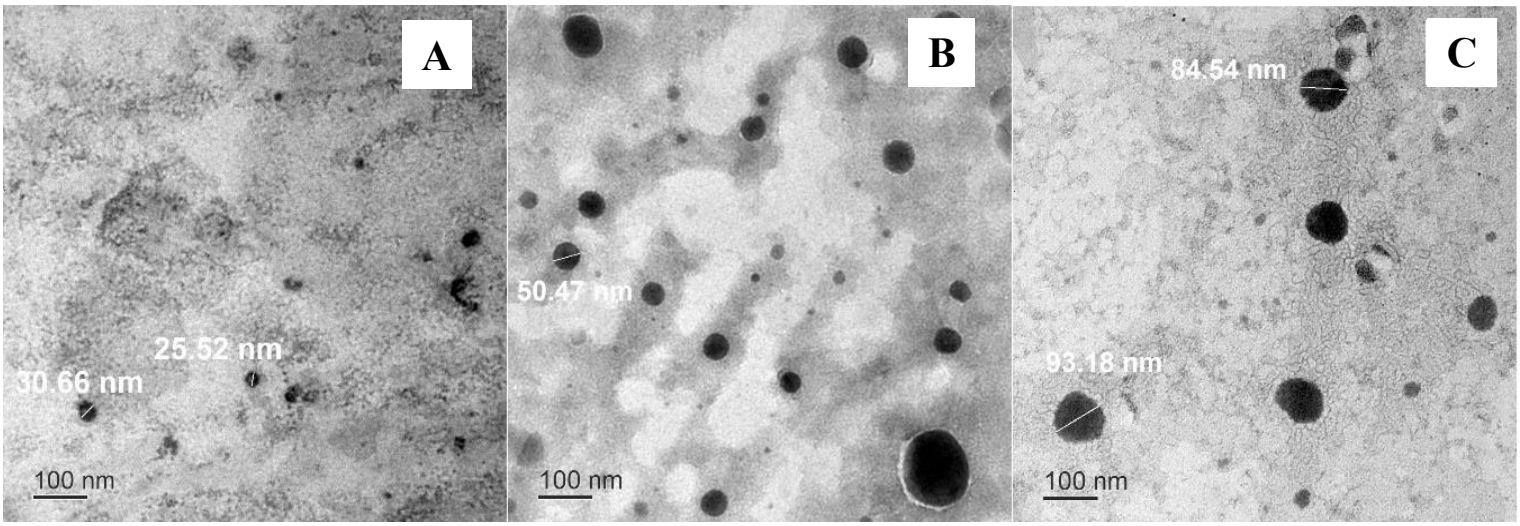

Figure 1. Morphological analysis of lipid nanocapsules by transmission electron microscopy. BNZ LNC A (A), BNZ LNC B (B) and BNZ LNC C (C). Bar = 100nm.

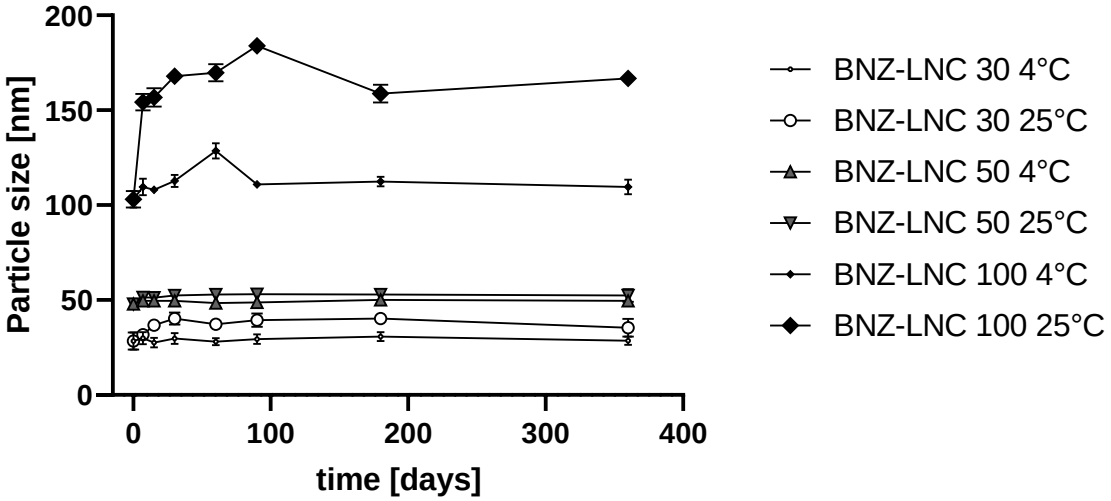

Figure 2. Storage stability of benznidazole lipid nanocapsules (BNZ-LNC) of 30 nm (30), 50 nm (50) and 100 nm (100) for 365 days at 4 ºC and 25 °C. All measurements were conducted in triplicates and data is represented as mean ± SD of n=9, from three independent experiments.

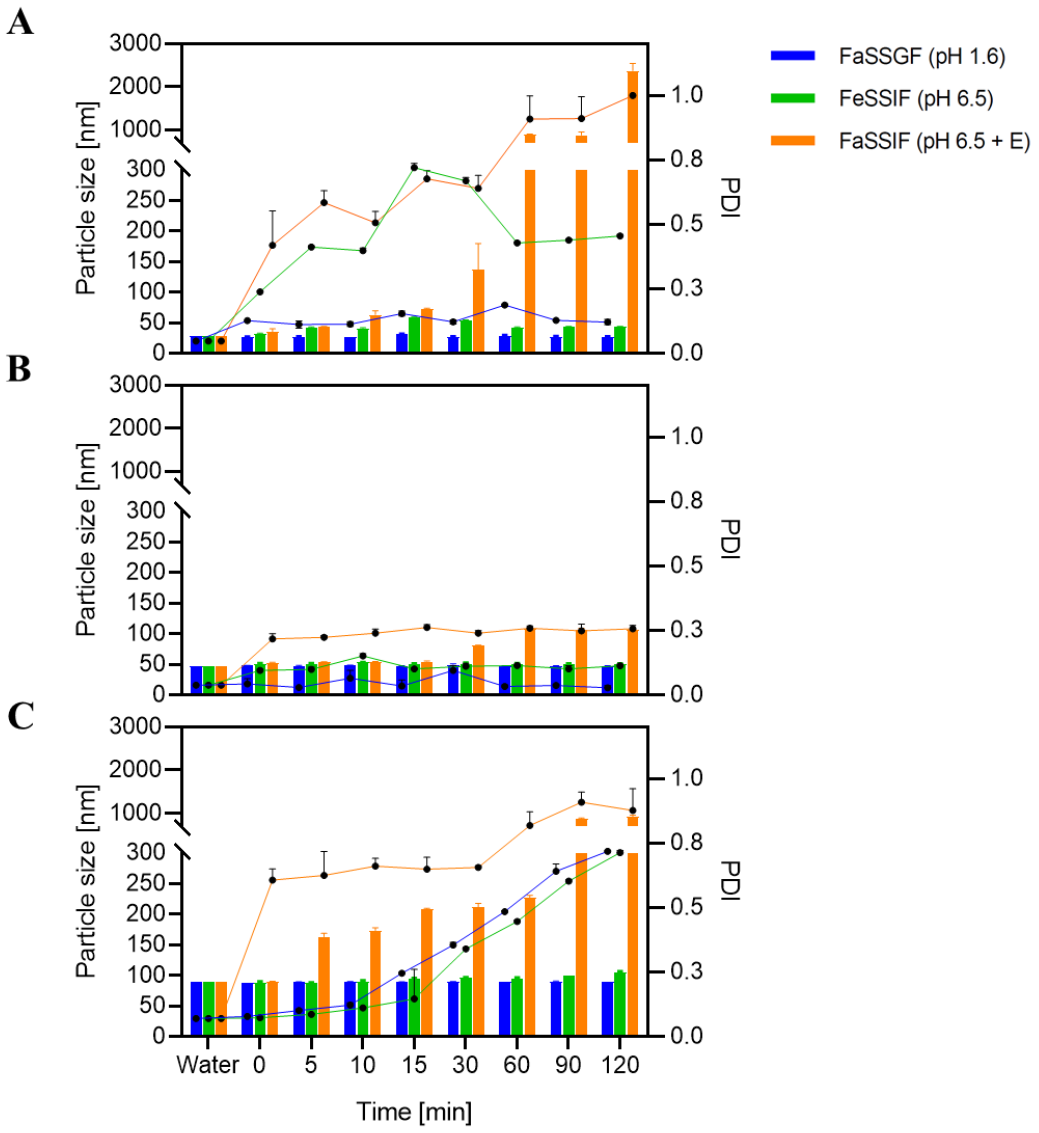

Figure 3. Stability of LNCs in simulated gastric and intestinal (GI) media: BNZ LNC A (A), BNZ LNC B (B) and BNZ LNC C (C) were incubated for 2 hours in fasted state simulated gastric fluid (FaSSGF), in fed state simulated intestinal fluid (FeSSIF) and in fasted state simulated intestinal fluid with pancreatic enzymes (FaSSIF+E). Bar graph represents particle size and line graph shows corresponding PDI. Data are shown as mean ± SD of n=9 of three individual experiments.

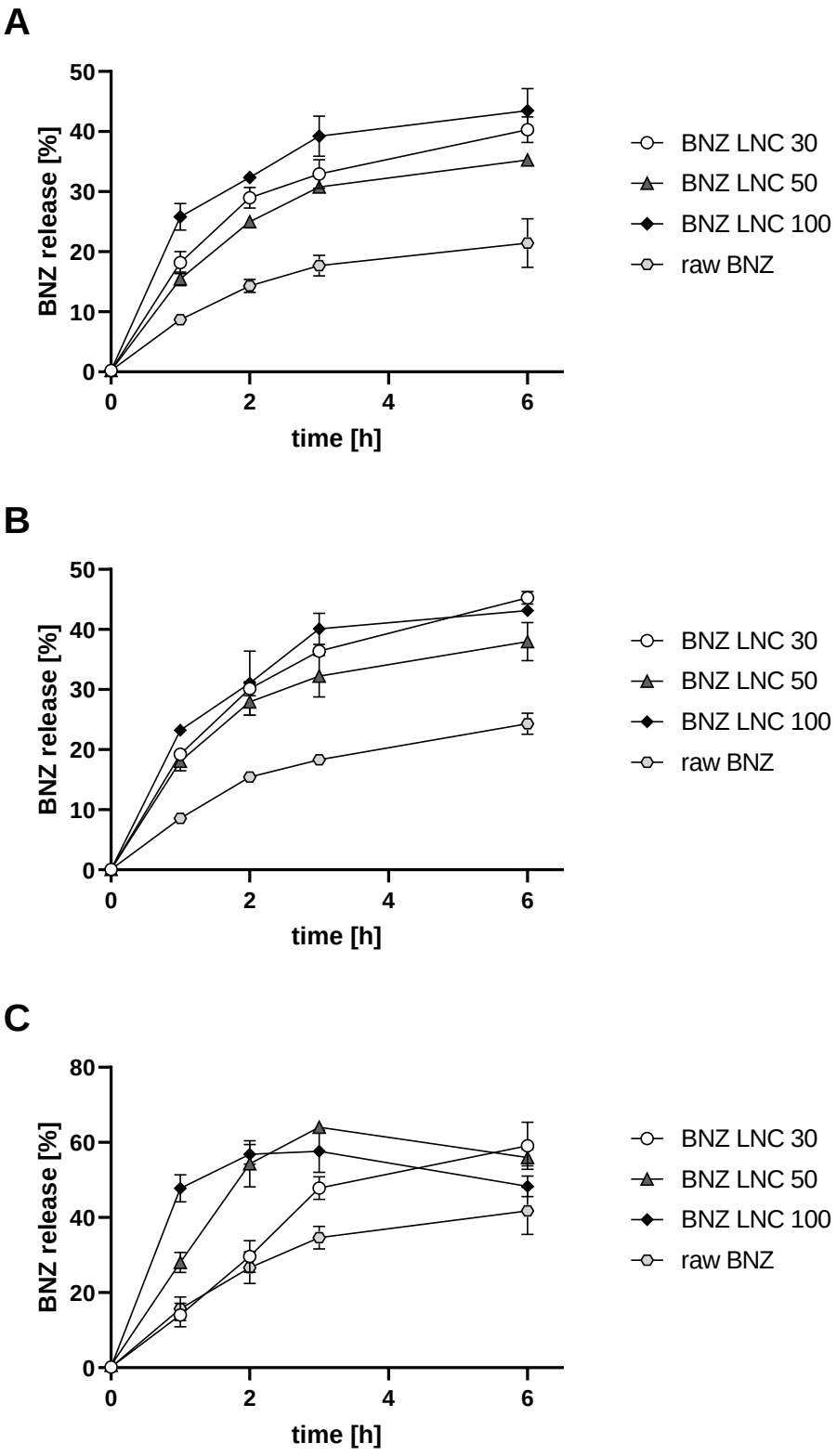

Figure 4. Cumulative benznidazole (BNZ) release from lipid nanocapsules (LNC) in different GI simulated media within 6h: FaSSGF pH 1.6 (**A**), FeSSIF pH 6.5 (**B**) and FaSSIF+E pH 6.5 with pancreatic enzymes (**C**). Data is represented as mean ± SD of n=9 from three individual experiments.

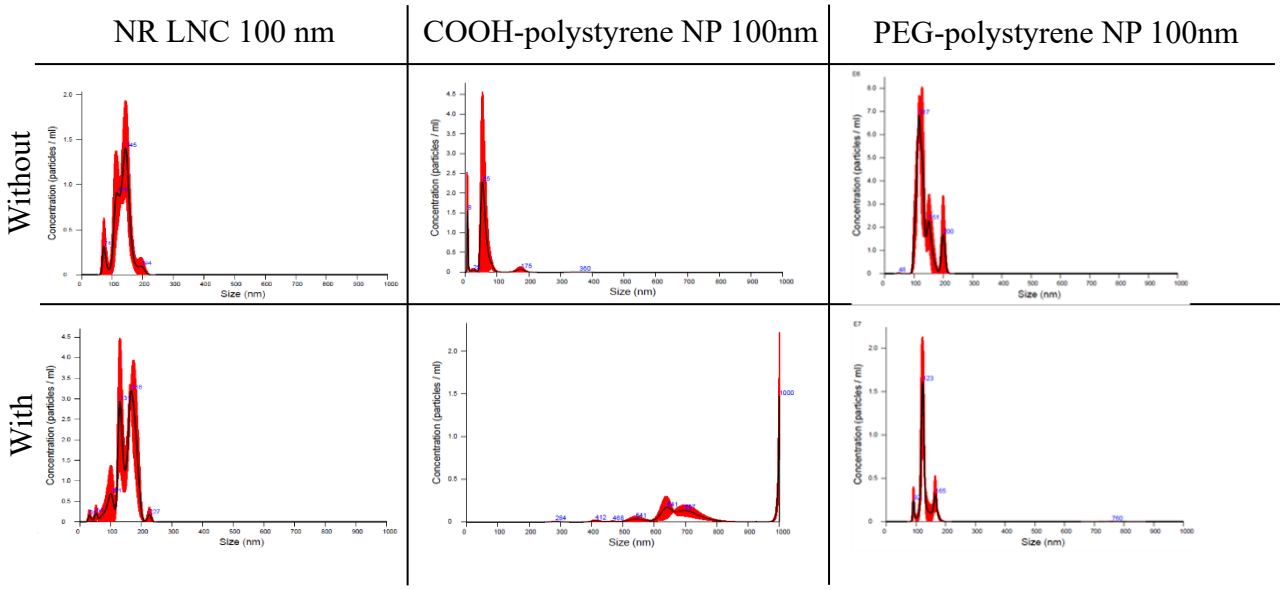

A

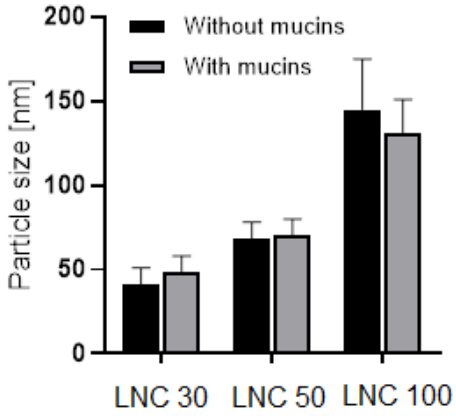

Figure 5. Particle size distributions of NR LNCs measured by NTA in presence or absence of mucins. Representative graphs of Nile Red (NR)-labeled LNC 100 compared to carboxylated and PEGylated polystyrene control NPs (100 nm) (**A**). Summary of mean particle size of all LNC formulations.

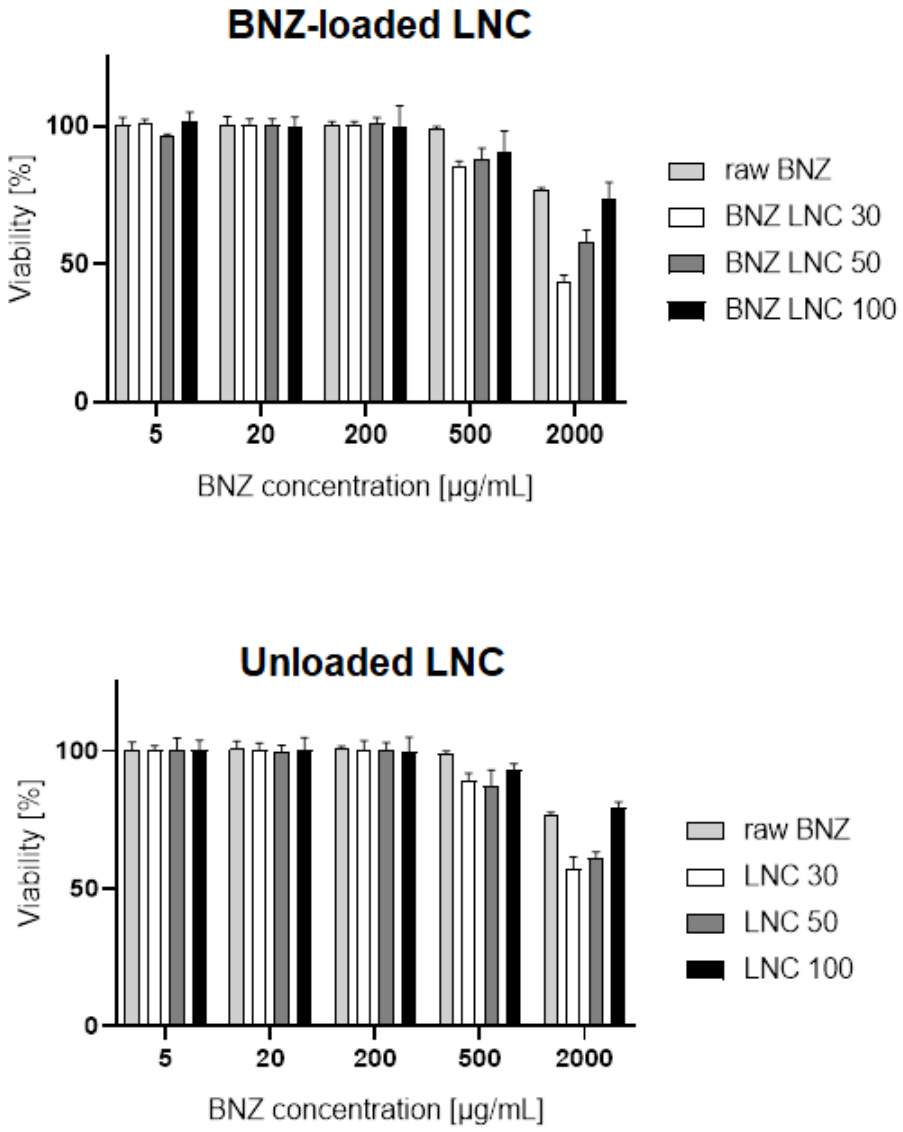

Figure 6. Cell viability of Caco-2 cells after incubation with benznidazole lipid nanocapsules (BNZ-LNC) and unloaded lipid nanocapsules (LNC) for 24h (MTT assay). Data are shown as mean ± SD of n=9 of three individual experiments.

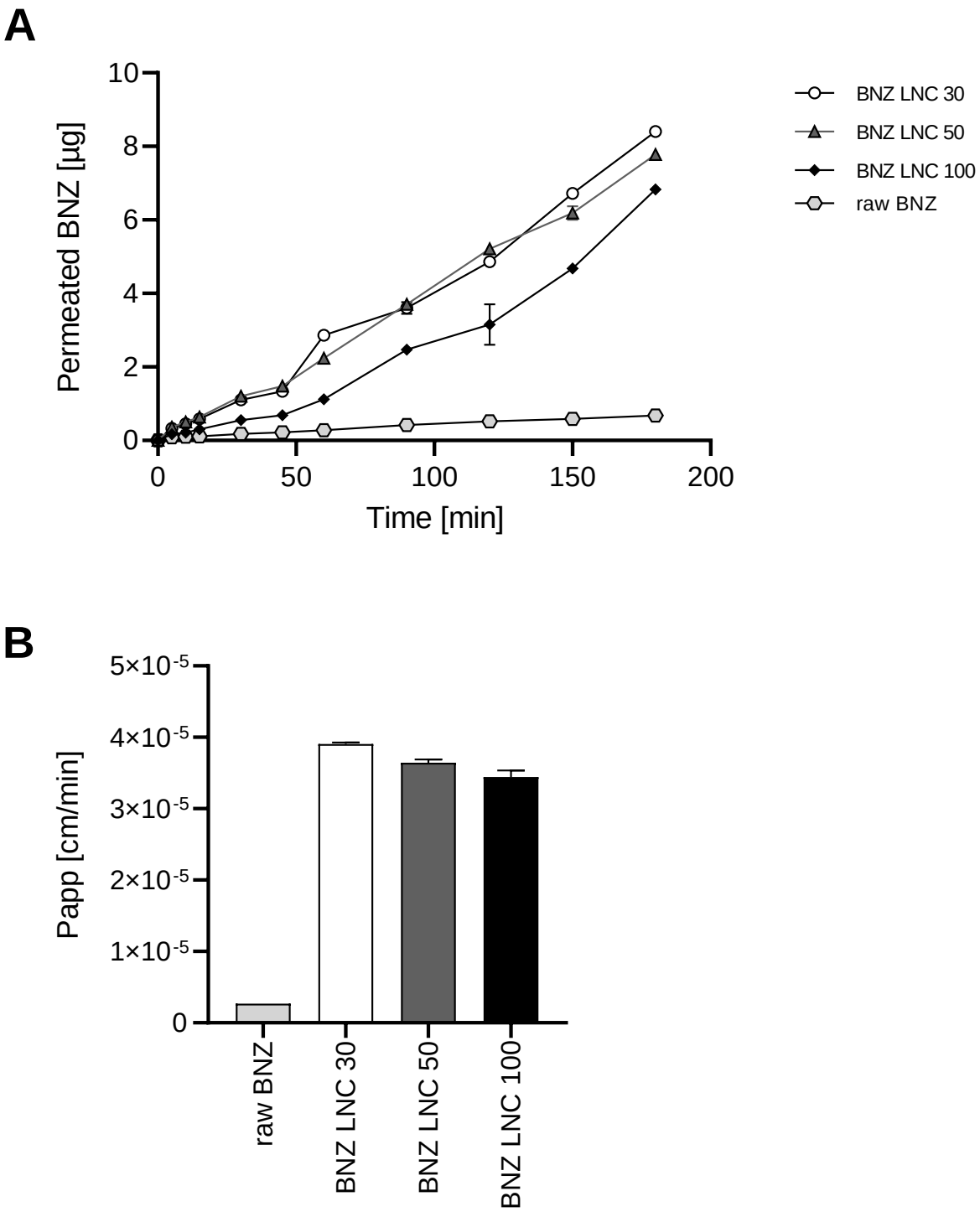

Figure 7. Permeation study of benznidazole lipid nanocapsules (BNZ-LNC) in Caco-2 cells. Cumulative amount of permeated benznidazole (**A**) and corresponding calculations of P_{app} value (**B**).

Supporting information (SI)

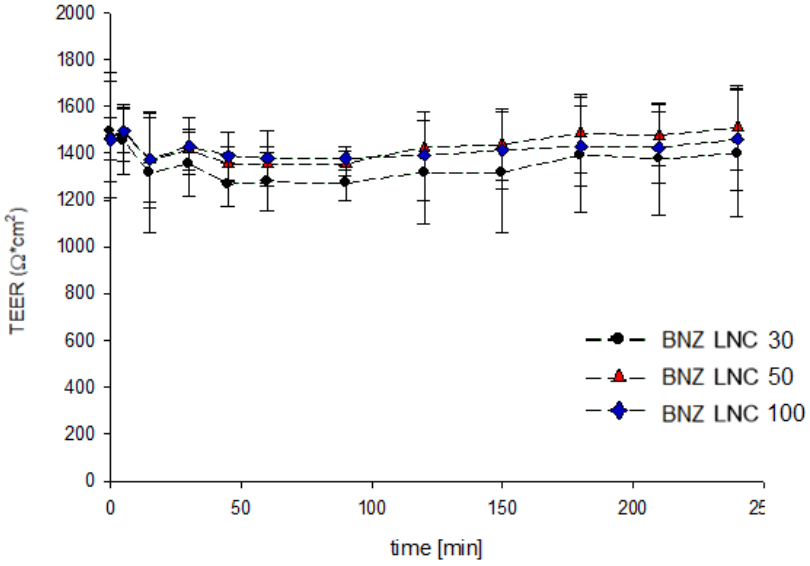

Figure 1-S. Epithelial integrity of Caco-2 cell layer during 6 h incubation of BNZ LNCs (Transepithelial electrical resistance: TEER).